

Detection of Radiation Therapy Induced Cerebral Microbleeds in Gliomas: Does High Field Mean High Yield?

Wei Bian^{1,2}, Christopher Hess¹, Susan Chang³, Sarah Nelson^{1,2}, and Janine Lupo¹

¹Radiology and Biomedical Imaging, University of California San Francisco, San Francisco, CA, United States, ²Joint Graduate Program in Bioengineering, University of California San Francisco & Berkeley, San Francisco, CA, United States, ³Neurological Surgery, University of California San Francisco

Introduction: Although radiation therapy is a mainstay in the treatment of patients with gliomas, it is estimated that approximately 60% of tissue within the high dose treatment field is normal brain tissue. Over time, this results in the formation of cerebral microbleeds (CMBs), focal perivascular collections of hemosiderin deposits, in normal brain tissue that persist for years after receiving radiation therapy¹. At lower field strengths, it has been shown that the detection of CMBs is enhanced with Susceptibility-weighted imaging (SWI) compared to T2*-weighted magnitude images², but there has been recent debate as to whether SWI is necessary at 7T where there is already heightened susceptibility in magnitude images. In addition, although studies have shown improved sensitivity to microbleeds on magnitude images at 3T and 7T compared to 1.5 T^{2,3}, it is not clear how much sensitivity is gained with 7T over 3T for CMB detection. The goal of this study, therefore, was to compare CMB detection between 3T and 7T field strengths and magnitude and SWI reconstructions in glioma patients with radiation-induced microbleeds.

Methods and Subjects: Ten patients with gliomas who had received radiation therapy between 2 and 15 years prior to the date of imaging, were scanned at both 3T and 7T GE scanners on the same day. High resolution T2*-weighted imaging using a 3D flow compensated SPGR sequence was performed at both field strengths with an 8-channel phased array receive coil. The TE/TR was 28/56ms at 3T and 16ms/50ms at 7T. A GRAPPA-based parallel imaging acquisition was implemented with either a 2-fold (3T) or 3-fold (7T) acceleration factor to keep total acquisition time within 6 minutes. Other parameters were the same for both scanners with flip angle 20°, 24cm FOV, and an in-plane resolution of 0.5 x 0.5mm, and 2mm slice thickness. The imaged volumes were carefully prescribed to ensure that the same coverage was obtained for both 3T and 7T scans. Standard SWI post-processing was performed on the reconstructed k-space data for each coil, and then combined and intensity corrected. Minimum intensity projection images through 8 mm-thick slabs were generated from both magnitude and SWI images and used for microbleeds identification. Microbleeds were identified as small hypointense foci that did not correspond to vessels on consecutive slices, and counted in normal-appearing tissue outside the tumor region. A Wilcoxon signed rank test was performed to test whether there was a significant difference in CMB detection between groups.

Figure 1. In a), a patient with tumor located in temporal lobe that extended to basal ganglia, where two CMBs (Yellow arrows) are seen on 3T SWI (Left) but masked by the high iron content of the globus pallidus on 7T SWI (Right). In b), a patient with a frontal lobe tumor, where one CMB (Red arrow) is detected by both 3T (Left) and 7T (Right) SWI, while the other (Yellow arrow) is only seen on 7T SWI. In c), 7T SWI identified 3 more CMBs (Yellow arrows) than the corresponding magnitude image.

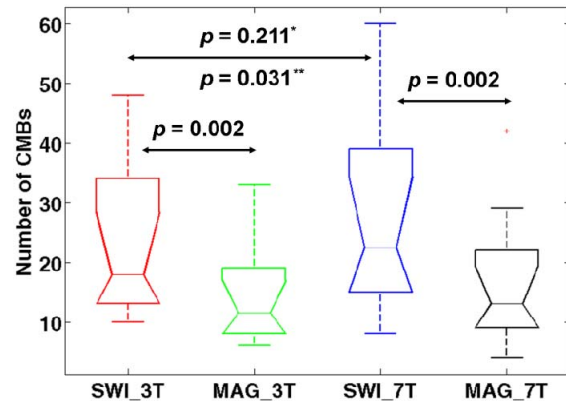
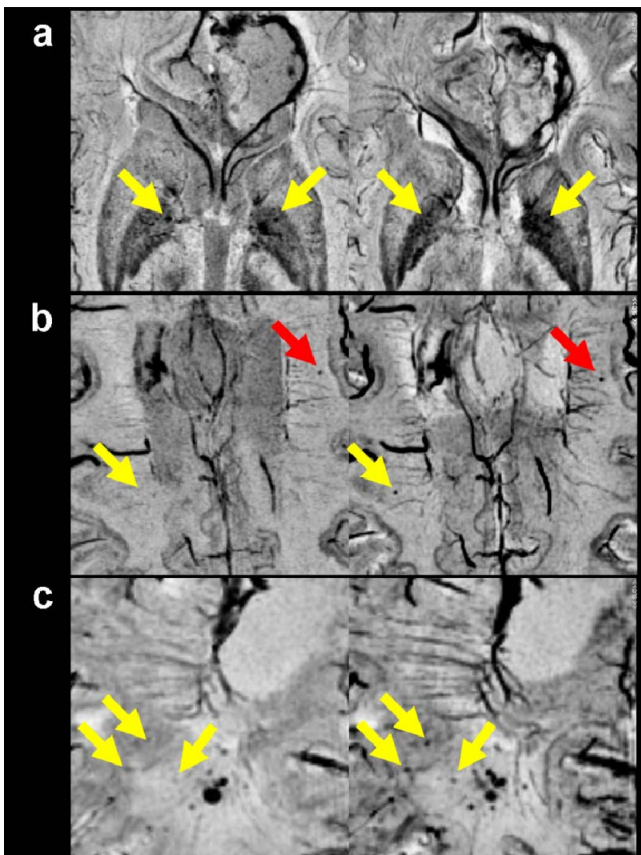


Figure 1. Box plots of the number of CMBs identified on SWI and magnitude images for all 10 patients at both 3T and 7T. * indicates the p value for the 10 patient comparison and ** is the p value for the 6 patient comparison after omitting 4 patients with tumors located in temporal lobe.

Results and Discussion: At 3T, a total of 226 (mean = 22.6; range 13~48) and 145 (mean = 14.5; range 8~33) CMBs were identified from all 10 patients on SWI and magnitude images, respectively, while 7T SWI and magnitude images detected 269 (mean = 26.9; range 8~60) and 164 (mean = 16.4; range 4~42) respective total CMBs (Figure 1).

7T vs. 3T SWI: Six out of ten patients had more CMBs identified on 7T SWI, while 3T SWI was able to detect more CMBs in three patients. One patient had an equal number of CMBs at both field strengths. Although this difference between field strengths did not achieve statistical significance, the three patients that had more CMBs at 3T had tumors that extended into the temporal lobe, suggesting that the decreased detection in these cases was due to heightened susceptibility artifacts near air-tissue interfaces. A representative example of this observation is shown on Figure 2(a). When comparing the 6 patients with frontal and parietal tumors, there was a statistically significant increase in microbleed detection at 7T compared to 3T ($p = 0.03$). Figure 2(b) shows a CMB from a patient that can be visualized at 7T but not at 3T with SWI, demonstrating the additional value of high field strength in CMB detection.

SWI vs. Magnitude at 7T: Similar to 3T, there was a significant difference ($p = 0.002$) in CMB detection between magnitude and SWI images at 7T, with a 64% higher detection rate with SWI compared to magnitude images. In addition, the contrast of CMBs to surrounding brain tissue was greatly improved, as shown in Figure 2(c). This heightened contrast is especially critical in visualizing radiation-induced CMBs, whose radii can be as small as 0.5 to 1mm, which is lower than CMBs observed in other diseases.

Conclusions: Although the sensitivity of CMB identification increases with field strength, the heightened susceptibility artifacts present at higher field strengths can limit their detection. In order to achieve the highest detection rate of CMBs for these patients, tumor location should be considered in conjunction with field strength. Even with the heightened sensitivity obtained at 7T, SWI is still beneficial in identifying microbleeds over conventional magnitude T2*-weighted GRE imaging.

References: 1. Lupo JM *et al.*, *Int J Radiat Oncol Biol Phys*. Epub 2011 Oct 12. 2. Nandigam RN *et al.*, *AJNR Am J Neuroradiol*. 2009;30(2):338-43.

3. Conijn MM *et al.*, *AJNR Am J Neuroradiol*. 2011;32(6):1043-9

This study was supported by UC Discovery grant ITL-BIO04-10148